A Promising Approach for Controlling the Second Coordination Sphere of Biomimetic Metal Complexes: Encapsulation in a Dynamic Hydrogen-Bonded Capsule

Tongtong Zhang, Laurent Le Corre, Olivia Reinaud, Benoit Colasson

FULL PAPER

A Promising Approach for Controlling the 2nd Coordination Sphere of Biomimetic Metal Complexes: Encapsulation in a Dynamic Hydrogen-Bonded Capsule

Tongtong Zhang,[a] Laurent Le Corre,[a] Olivia Reinaud[a] and Benoit Colasson*[a]

[a] T. Zhang, Dr. L. Le Corre, Pr. O. Reinaud, Dr. B. Colasson
Université de Paris
UMR 8601, CNRS
45 rue des Saints Pères, F-75006 Paris, France
E-mail: benoit.colasson@parisdescartes.fr

Supporting information for this article is given via a link at the end of the document.

Abstract: The design of biomimetic models of metalloenzymes needs to take into account many factors and is therefore a challenging task. We propose in this work an original strategy to control the second coordination sphere of a metal centre and its distal environment. A biomimetic complex, reproducing the first coordination sphere, is encapsulated in a self-assembled hydrogen-bonded capsule. The cationic complex is co-encapsulated with its counter-anion or with solvent molecules. The capsule is dynamic allowing a fast in/out exchange of the co-encapsulated species. It also provides a hydrogen-bonding site in the second coordination sphere. The capsule is also a source of proton as it can be deprotonated in presence of the complex providing a globally neutral host-guest assembly. This simple and broad scope strategy is unprecedented in biomimetic studies. It appears as a very promising method for the stabilisation of reactive species and for the study of their reactivity.

Introduction

Metalloenzymes are ubiquitous and responsible for a wide range of challenging chemical transformations under mild conditions and with high chemo-, regio- and stereo-selectivities.[1] The development of synthetic models is a long standing endeavor.[2] These artificial models are designed to mimic molecular aspects of the biological catalysis within an active site in order to gain access to fundamental information about the mechanisms at work. Ultimately, it can lead to the development of bio-inspired catalysts which operates with benign reactants (e.g. O_2 as the oxidant) and the discovery of new reactivity patterns. Classically, the models reproduced the first coordination sphere around the metal ion (nature and number of the coordinating atoms, denticity of the ligand and geometry of the metal complex). However, these models lack several important features of enzymes. Indeed, the active site in the enzyme cannot be reduced to its metal cofactor and the amino acid residues directly bound to it. The enzyme pocket plays a key role for the control of the nuclearity, the substrate binding, the substrate/catalyst/reactant pre-association, the regio- and stereo-selectivities and the substrate-product in⇆out exchanges. It also provides a well-defined second coordination sphere for the activation and/or stabilisation of intermediate reactive species and protects the metal centre from undesired pathways. A second coordination sphere can be introduced directly on the ligand.[3-8] However it does not address most of the other aspects of the enzymatic catalysis. Other strategies based on the association of a biomimetic coordination core and a cavity aiming at reproducing the influence of the enzymatic binding pocket have been proposed: i) the “more” biomimetic strategy is based on the grafting (either covalently or not) of a metal coordination complex to an apoprotein[9] or the production of *de novo* designed proteins offering a well-defined cavity around the metal ion[10]; ii) in line with the first strategy, DNA is another valuable biomolecule that has been tested. It provides a chiral second coordination sphere around an intercalated metal complex and influences for instance stereoselective reactions[11]; iii) a metal complex is covalently grafted in close proximity to a cavity (cyclodextrine, calixarene, resorcinarene,…) allowing a strong communication between the metal centre and the cavity space.[12] All these studies have validated the hypothesis that the presence of an enzyme pocket mimic can lead to rate acceleration, substrate selectivity, regio- or stereoselectivity or intermediate stabilisation. Nevertheless, these strategies suffer from major drawbacks of using fragile or synthetically time consuming building blocks.

Interestingly, other approaches for the encapsulation of transition metal catalysts have been explored. All these approaches have in common to encapsulate a metal complex within a self-assembled molecular cage. The encapsulation can be driven by template-ligand methods (i.e., in some ways, the first coordination sphere of the metal complex is attached to the molecular capsule)[13] or by a host-guest process (the metal complex is held in the cavity of the capsule by non-covalent interactions).[14] Examples following the latter strategy are still very limited mostly because the use of very large molecular capsules is required. The Fujita group has reported some examples of cationic self-assembled coordination cages.[15] The Raymond and Toste groups have intensively studied the encapsulation of metal complexes in anionic tetrahedral coordination cages and have highlighted host-selective reaction pathways.[16-19] Other examples make use of a capsule assembled from six resorcin[4]arene molecules and 8 water molecules held together by a large network of hydrogen bonds.[20] Hence, the groups of Reek and Scarso established that the encapsulation in this capsule of a monocationic NHC-gold complex influenced its catalytic activity.[21] A few years later, more in-depth studies about the structural characterisation of this

supramolecular catalyst were reported.[22] Most of the systems based on a direct encapsulation published to date deals with organometallic complexes (Pd, Rh, Au). This encapsulation strategy has been operated for biomimetic model complexes only in a unique but promising example of a Mn-porphyrin embedded in a micelle-like molecular capsule.[23] It was demonstrated that during the epoxidation of styrene the encapsulation stabilised the Mn-oxo reactive species and enforced the proximity between the catalyst and the substrate. Hence, further studies on biomimetic models based on the encapsulation of complexes spanning from their characterisations to catalysis are required.

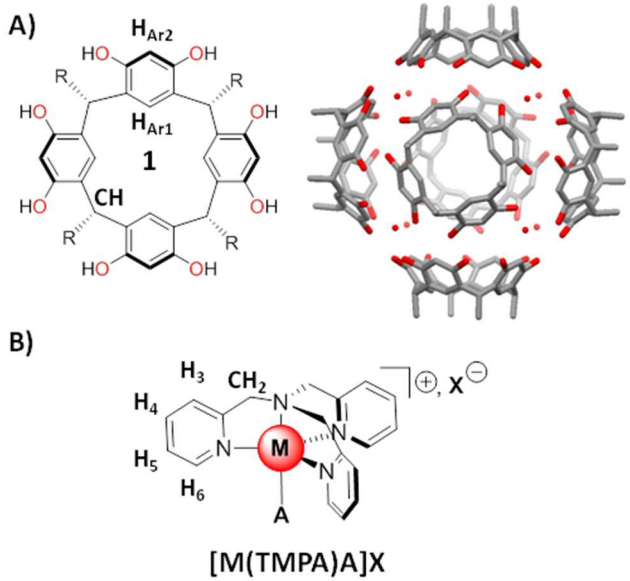

Figure 1. A) Molecular structure of the resorcin[4]arene **1** used in this study (R = $C_{11}H_{23}$) and X-ray structure of the hexameric capsule $\mathbf{1_6}$ (obtained with R = CH_3; carbon atoms are in grey and oxygen atoms in red; the hydrogen atoms are omitted for clarity)[20]; B) Molecular structure of the biomimetic monocationic TMPA complexes **[M(TMPA)A]X** (**M**$^{2+}$ = Zn^{2+}, Cu^{2+}; **A**$^-$ = Cl^-, N_3^-; **X**$^-$ = ClO_4^-, $CF_3SO_3^-$, $BArF^-$, $[(ZnCl_4)_{1/2}]^-$) The protons are labeled and these labels are used for the description of the NMR spectra.

As a first step, we wish to report on the encapsulation of well-known bioinorganic model complexes based on the tris(2-pyridylmethyl)amine (TMPA) ligand[24] within the self-assembled hexameric resorcin[4]arene capsule (Figure 1). This capsule is composed of readily available resorcin[4]arene units **1**.[20] It is formed by the spontaneous assembly of six resorcinarenes and 8 water molecules ($\mathbf{1_6.8H_2O}$, referred to as $\mathbf{1_6}$ for simplicity) in a water-saturated non polar organic solvent (e.g. $CHCl_3$, benzene) (Figure 1A, S1 and S2). The structure holds thanks to 60 hydrogen bonds. The inner cavity with a volume of 1375 Å^3 is large enough to encapsulate 8 benzene molecules or 6 chloroform molecules offering the possibility to sterically accommodate a metal coordination complex. As a matter of fact, it was shown that this capsule can encapsulate different metal complexes such as ferrocenium,[25] cobaltocenium,[26] Ru(II)-trisbipyridine,[27,28] cyclometallated Ir(III) complex.[29] Moreover, in the case of the cationic gold(I) carbene complex above mentioned, the influence of the encapsulation on the outcome of a catalytic hydration of alkynes was proved.[21] Noteworthily, in the context of organocatalysis, the same capsule has often been employed.[30,31] Hence, this capsule is able to encapsulate large coordination complexes and to play a role in (metal-) catalysed processes. Indeed, the encapsulation is thermodynamically driven and is highly dynamic, allowing in⇆out exchanges for the substrates and the products. For these reasons, it appears as a good candidate to study the encapsulation of bioinorganic models. Many biomimetic model complexes have been studied over the years. Among them, complexes based on TMPA have proved to be very useful to obtain valuable information (e.g. in Cu^I-O_2 chemistry).[32-35] TMPA ligand has a rich coordination chemistry and several metal complexes [e.g. Cu^I, Cu^{II}, Zn^{II}, Fe^{II}, Co^{II}] can be obtained.[24]

Results and Discussion

In this study we focused on monocationic complexes **[M(TMPA)A]X** (M = Zn^{II}, Cu^{II}; A^- = Cl^-, N_3^-; X^- = ClO_4^-, $CF_3SO_3^-$, $BArF^-$ [$BArF^-$ = tetrakis(3,5-bis(trifluoromethyl)phenyl)borate], $[(ZnCl_4)_{1/2}]^-$) based on the non-functionalised TMPA ligand (Figure 1B) (see the Supporting Information for their synthesis and characterisation, Figures S3 to S20). These complexes are five-coordinate and adopt a trigonal bipyramidal geometry. We were particularly interested in evaluating i) the influence of the counter-anion X^- on the encapsulation process, ii) the interactions at play between the complex and the hexameric capsule, iii) the exchange of co-encapsulated species within the assembly and iv) the effect of the deprotonation of the capsule on the assembly.

Role of the counter-anion

In previous studies on the encapsulation of monocationic ammonium salts in capsule $\mathbf{1_6}$, the role of the counter-anion was proved to be crucial. The co-encapsulation of the anion (often a halide anion) with the cation was proposed as one of the driving force for the recognition of the ammonium.[36] More recently, it was proposed that upon encapsulation of a hydronium cation, the anion could replace one of the 8 water molecules in the assembly.[37] Yet, some examples of encapsulation of the sole cationic part with the separation of the ion pair were also notified.[21,22,27,28] Thus, the role of the anion is not yet fully understood and seems at least to be cation dependent.

BArF counter anion. The encapsulation was first examined by NMR spectroscopy with the diamagnetic complex **[Zn(TMPA)Cl]BArF**. The $BArF^-$ anion is too large to be co-encapsulated with the monocationic $[Zn(TMPA)Cl]^+$ species. Moreover, it forms a loose ion pair, which should not jeopardise the encapsulation of the cation because of a too high energetic penalty due to the dissociation of the ion pair. A 1:1 mixture of **[Zn(TMPA)Cl]BArF** and $\mathbf{1_6}$ was studied in water-saturated $CDCl_3$. The ^{1}H NMR spectrum recorded just after the mixing mostly consisted in the superimposition of the two initial species with only traces of a new species (Figure S21). The evolution of the spectrum was slow and required more than 5h at 50°C to be complete. After 18h at this temperature, the resonances of the free complex completely disappeared, new resonances emerged at a higher field and the initial resonances of the aromatic protons H_{Ar1} and H_{Ar2} of $\mathbf{1_6}$ were slightly shifted (Figure 2). DOSY experiments confirmed that the capsule remained intact since the diffusion coefficient measured for the 1:1 mixture and for the capsule alone are close and in agreement with the value

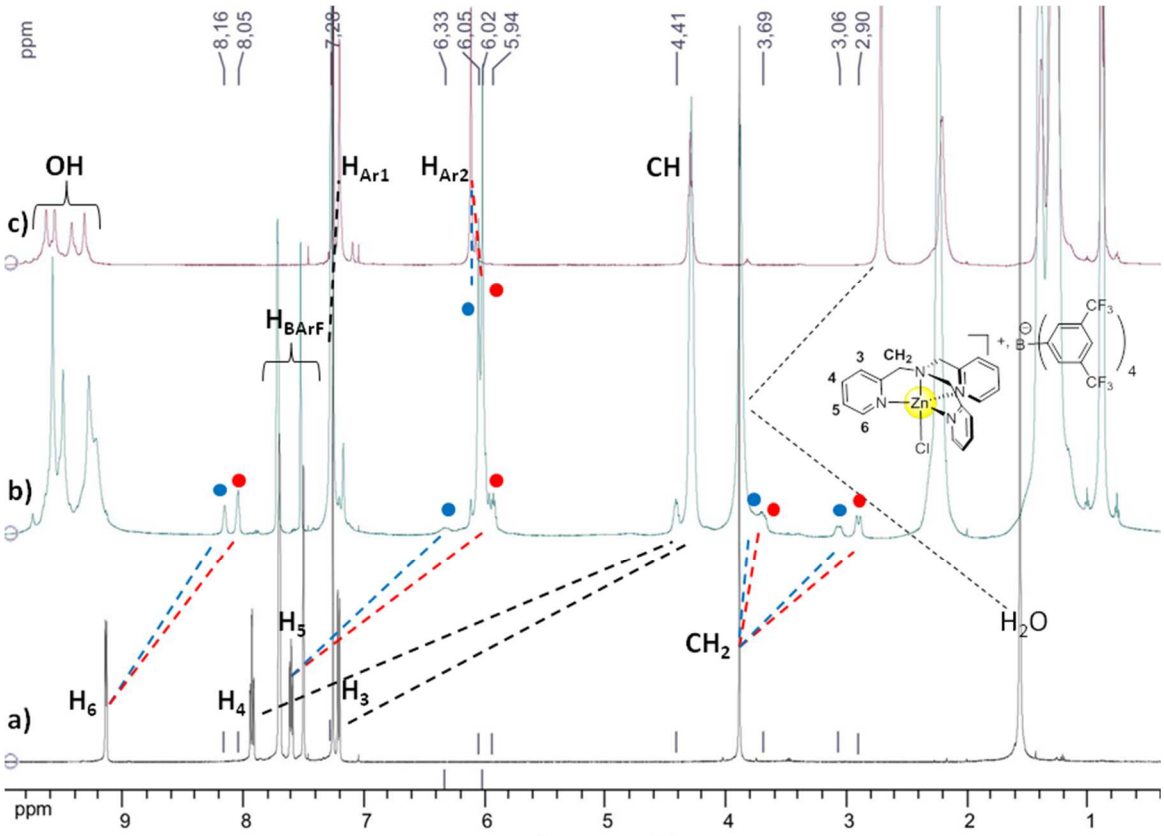

Figure 2. ^{1}H NMR spectra (water-saturated $CDCl_3$, 300 K, 500 MHz) of a) **[Zn(TMPA)Cl]BArF**, b) a 1:1 mixture at 4 mM of **[Zn(TMPA)Cl]BArF** and capsule $\mathbf{1_6}$ after 18 h at 50°C and c) capsule $\mathbf{1_6}$. The proton labeling referred to Figure 1. When possible, the peaks for the two diastereomeric assemblies are marked with red or blue dots.

reported earlier (Figure S22).[37] Importantly, the new resonances share the same diffusion coefficient indicating that they belong to a new species encapsulated in $\mathbf{1_6}$. Indeed, they are upfield shifted compared to the free complex, which is best explained by the shielding effect of the resorcinol rings. In contrast, the chemical shifts of the $BArF^-$ anion are not shifted proving that the anion is not encapsulated. In the spectrum recorded after 2h at 50 °C (Figure S21) the co-existence of the resonances for the free and encapsulated complexes indicates a slow in⇆out exchange rate of the complex on the spectroscopic timescale as already reported for other guests.[38] The attribution of the new peaks was completed by COSY and HSQC experiments (see SI for a detailed discussion). On the ^{1}H NMR spectrum, two sets of signals correspond to two different encapsulated complexes (blue and red dots in Figure 2). In addition, both complexes present diastereoisotopic CH_2 protons meaning that they both sit in a chiral environment. This is due to the fact that capsule $\mathbf{1_6}$ is present in solution as a mixture of diastereomers, some of them being chiral, differing in the orientation of the hydroxyl groups in the hydrogen-bond network covering the surface of the capsule.[20] Hence, **[Zn(TMPA)Cl]BArF** is encapsulated in two different diastereomers of $\mathbf{1_6}$ both of them being chiral.[22] These two diastereomers **[Zn(TMPA)Cl@1$_6$]BArF** are in slow exchange at room temperature.

To address the question of the presence of co-encapsulated solvent molecules, we repeated the NMR experiments with a 1:1 mixture of **[Zn(TMPA)Cl]BArF** and $\mathbf{1_6}$ in protiated chloroform. The ^{1}H NMR spectra taken just after the dissolution or after 18 h at 60°C are identical to the one recorded in deuterated chloroform except for the presence of a new set of signals. Just after the dissolution, the encapsulation of the complex is still limited and $\mathbf{1_6}$ mostly contains 6 $CHCl_3$ molecules which are attested by some signals at ca. 5 ppm as previously observed by Rebek et al. (Figure S27).[39] After the full encapsulation of the complex, this set of signals is no longer present and a new signal at 6.19 ppm appears (Figure S28). Since this peak is not observed in $CDCl_3$, it can be attributed to the encapsulated solvent molecules and its integration shows that approximately 3 chloroform molecules are co-encapsulated with the cation (Figure S29).

Perchlorate and triflate counter-anions. Two other smaller counter-anions were tested. The complexes **[Zn(TMPA)Cl]ClO$_4$** and **[Zn(TMPA)Cl]OTf** were dissolved in water-saturated $CDCl_3$ in presence of one equivalent of $\mathbf{1_6}$. In both case, the full encapsulation was detected immediately after the mixing and was confirmed by ^{1}H, COSY and HSQC NMR experiments. The ^{1}H NMR signals for the assemblies with the perchlorate or triflate complexes indicate mostly a symmetrical species but while only one major isomer is detectable by looking at the CH_2 region for the triflate case, up to three isomers are present for the

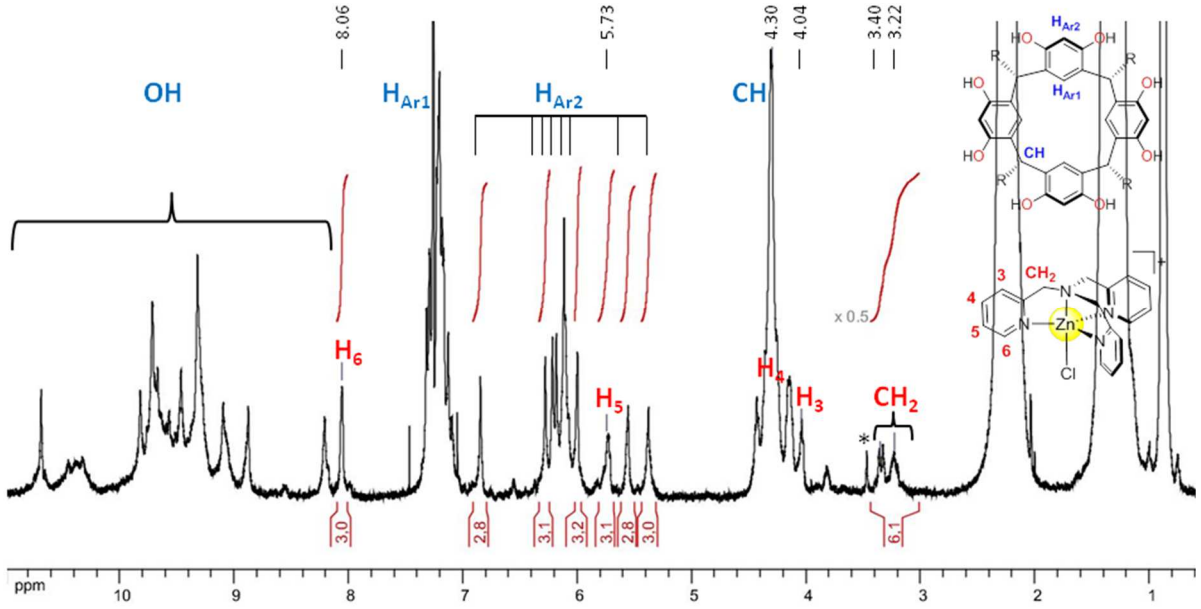

Figure 3. ^{1}H NMR spectrum (water-saturated $CDCl_3$, 300 K, 500 MHz) of a 1:1 mixture at 1 mM of **[Zn(TMPA)Cl](ZnCl$_4$)$_{1/2}$** and capsule **1$_6$** (* indicates a contamination with CH_3OH).

perchlorate (Figures S30 to S35). Interestingly, ^{19}F NMR experiments show that the chemical shift for the triflate anion is shifted by ca. + 1 ppm in presence of the capsule, indicating the possible co-encapsulation of the triflate anion (Figure S36).

Halide counter-anions. A halide anion, as mentioned in the literature, can be co-encapsulated or can replace one of the 8 water molecules. In any cases, the interaction of the anion with the capsule is assigned to its size and ability to form hydrogen-bond(s) with some elements of the capsule (either a water molecule or hydroxyl groups of the resorcinarenes). We anticipated that the nature of the halides, their size and hydrogen bond accepting capability would influence the final assembly. To probe this effect, 1.3 eq of a tetrabutylammonium salt (NBu_4F, NBu_4Cl, NBu_4Br or NBu_4I) were added into a 3 mM solution of **[Zn(TMPA)Cl@1$_6$]BArF**. In each case, a complete modification of the ^{1}H NMR spectrum was detected just after the addition (Figure S37). These spectra did not evolve further upon heating at 50°C during several hours. The 4 spectra are not fully superimposable. For instance, in the negative region, the intensities of the peaks are slightly different, attesting more or less encapsulation of the ammonium (*vide infra*). This trend corresponds to the different stability for **[NBu$_4$-X@1$_6$]** as a function of the halide as already reported.[38] Nevertheless, they all share similar features: i) the spreading of the OH region over more than 3 ppm (even 5 ppm for X^- = F^-) and ii) the splitting of the peak for H_{Ar2} around 6 ppm. From this experiment, no obvious difference between the 4 halide anions can be established. ^{19}F NMR experiments performed with NBu_4F show a large shift of the resonance of the fluoride anion (from -128.9 ppm for NBu_4F to -113.0 ppm in presence of the encapsulated complex) and indicate an interaction between the capsule and the anion (Figure S38). These anions seem to be equally involved in the final assembly **[Zn(TMPA)Cl-X@1$_6$]**, the legitimate interpretation being that they are either co-encapsulated or part of the capsule itself by replacing a water molecule. At this stage, the origin of the complexity of these ^{1}H NMR spectra remained unclear. Two hypotheses are plausible: the complexity is due to a loss of symmetry of the **[Zn(TMPA)Cl-X@1$_6$]** assembly or the halide anion gives a mixture of more than the 2 observed diastereomers for **[Zn(TMPA)Cl@1$_6$]BArF**.

This question could be solved by the in-depth NMR analysis of the encapsulation of the complex **[Zn(TMPA)Cl](ZnCl$_4$)$_{1/2}$**. A 1:1 mixture of this complex with **1$_6$** was analyzed by ^{1}H NMR spectroscopy just after the mixing (Figure 3). Besides the absence of the peaks for the $BArF^-$ and the ammonium species,[40] the spectrum is identical to the one corresponding to **[Zn(TMPA)Cl@1$_6$]BArF** in presence of Bu_4NCl (Figure S39). In contrast to what was observed with **[Zn(TMPA)Cl]BArF**, full encapsulation was fast and the ^{1}H NMR spectrum did not change upon heating the sample at 50 °C during several hours. This spectrum can be explained by the presence of a pool of "free" chloride anions available in the anion $(ZnCl_4)^{2-}$. In presence of the capsule, the following equilibrium involving this anion is shifted to the right (possibly driven by the precipitation of $ZnCl_2$ even if no precipitate was observed with naked eye) and leads to the co-encapsulation of the chloride:

[Zn(TMPA)Cl@1$_6$](ZnCl$_4$)$_{1/2}$ ⇆ **[Zn(TMPA)Cl-Cl@1$_6$]** + ½ $ZnCl_2$

To test the hypothesis of the co-encapsulation of the chloride anion, another experiment was performed. To the 1:1 mixture containing **[Zn(TMPA)Cl](ZnCl$_4$)$_{1/2}$**.and **1$_6$** previously obtained, 2 equivalents of AgOTf were added. After heating at 50 °C, a precipitate was formed and the initial

^{1}H NMR spectrum had disappeared for the benefit of a new spectrum identical to the one independently obtained when **[Zn(TMPA)Cl]OTf** was mixed with **1_6** (Figure S40). In presence of the silver cation, the precipitation of $AgCl_s$ drives the following reaction to completion:

[Zn(TMPA)Cl-Cl@1_6] + ½ $ZnCl_2$ + 2 AgOTf → **[Zn(TMPA)Cl@1_6]OTf** + ½ $ZnOTf_2$ + 2 $AgCl_s$

Hence, it appears that the use of the complex **[Zn(TMPA)Cl]$(ZnCl_4)_{1/2}$** to study the encapsulation in **1_6** is a synthetically available equivalent of the complex **[Zn(TMPA)Cl]Cl**. The encapsulation of the cation $[Zn(TMPA)Cl]^+$ occurs together with the interaction of the chloride anion with **1_6**. The complete characterisation of the assembly **[Zn(TMPA)Cl-Cl@1_6]** and the attribution of the ^{1}H NMR spectrum (Figure 3) could be achieved with additional DOSY, HSQC, COSY and ROESY NMR experiments (see SI for a detailed discussion). This NMR study allows for proposing a mode of interaction between the cation and the capsule. The hexameric capsule can be schematically represented as a cube, the 6 faces of which are occupied by a resorcinarene macrocycle and the 8 vertices by a water molecule (Figure 4). In this cube, $[Zn(TMPA)Cl]^+$ sits in one corner with each pyridine being in interaction with the cavity of one resorcinarene, i.e. pointing in the direction of one of the 3 faces (faces A in Figure 4). At this point, two orientations of the cation can be envisaged. In the first one (Figure 4A), the Zn-chloride vector points towards the centre of the cube while for the second orientation this vector is orientated towards one corner of the cube (Figure 4B).

In both cases, the resorcinarenes are divided in two groups. The resorcinarenes capping the faces A have their cavities occupied by a pyridine ring while the resorcinarenes over the faces B are “empty”. For a given resorcinarene of one of these two groups then, each H_{Ar2} protons is chemically different ($H_{Ar2a\text{-}a'}$, $H_{Ar2b\text{-}b'}$, $H_{Ar2c\text{-}c'}$, and $H_{Ar2d\text{-}d'}$). This mode of interaction is consistent with the presence of 2×4 = 8 resonances for H_{Ar2}.

The full encapsulation of the cation $[Zn(TMPA)Cl]^+$ is observed with all four counter-anions used in this work. The encapsulation of the cation is possible with (halides, OTf^-) or without ($BArF^-$) the co-encapsulation of the anion. The encapsulation is slower for the $BArF^-$ anion compared to Cl^- (initially present in $(ZnCl_4)^{2-}$), ClO_4^- and OTf^-. The ^{1}H NMR spectra disclose the presence of up to three major highly symmetrical diastereomeric host-guest complexes (for $BArF^-$, ClO_4^-, OTf^-) or the presence of one major isomer with a lower symmetry (for halides). When the anion sits outside of the capsule, three $CHCl_3$ molecules are co-encapsulated. The chloride anion can be replaced by a triflate anion showing that guest exchange is possible. In spite of these different ^{1}H NMR patterns and the presence or absence of co-encapsulated anion, the rather similar chemical induced-shift (CIS) values measured for the four complexes (Table S1)[41] advocate for an equivalent position of the cation inside the capsule. The protons H_3 and H_4 have the largest CIS (~ - 3.5 ppm for both protons) implying a smaller average distance between these two protons and the shielding regions of the resorcinarenes when compared to the other protons of the complexes. These observations also suggests that more than the position of the cation $[Zn(TMPA)Cl]^+$ inside the capsule, the presence of the chloride anion modifies the dynamics of its tumbling motion.

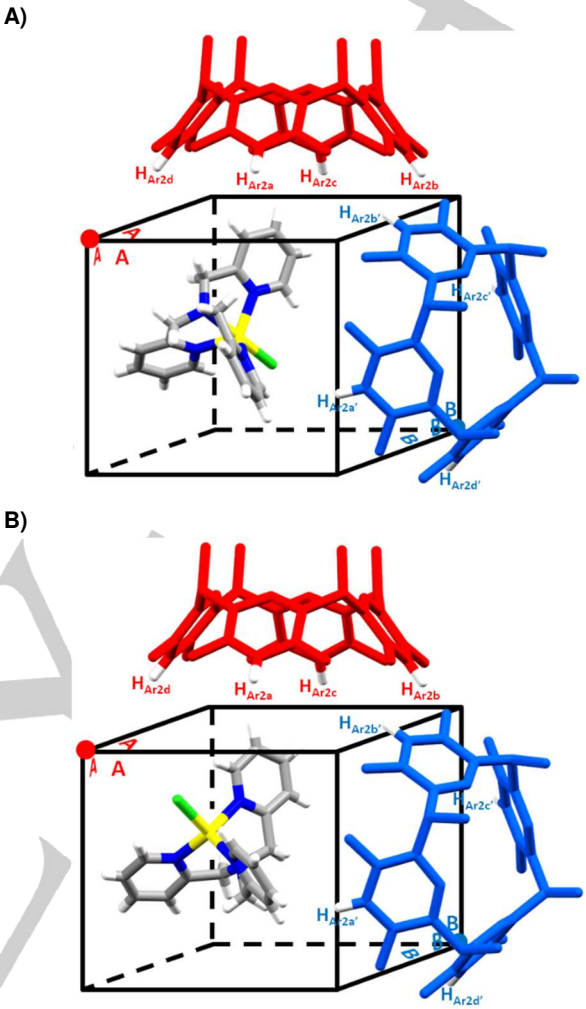

Figure 4. Schematic representation of the two possible positions of the $[Zn(TMPA)Cl]^+$ cation inside the capsule according to the analysis of the NMR data for **[Zn(TMPA)Cl-Cl@1_6]**. The 6 resorcinarenes units are divided in two groups: group A in red when the cavity is occupied by a pyridine unit and group B in blue when the cavity is empty. The protons of the complex and the protons H_{Ar2} of the resorcinarene are represented in white.

Docking of $[Zn(TMPA)Cl]^+$ inside 1_6

To have more insights about the preferred positions of the cation, we performed some molecular modeling by docking the cation $[Zn(TMPA)Cl]^+$ inside **1_6** using LigandFit.[42] The docking of $[Zn(TMPA)Cl]^+$ inside **1_6** was realised in absence of the anion or additional $CHCl_3$ molecules since the analysis of the NMR spectra revealed that its position was conserved for all the complexes.

Two almost isoenergetic binding poses were found (Figure 5). These two poses are very similar to the one proposed by the NMR analysis in Figure 4. In the first one (pose A Figure 5 left and Figures S53 and S54), the Zn-Cl vector

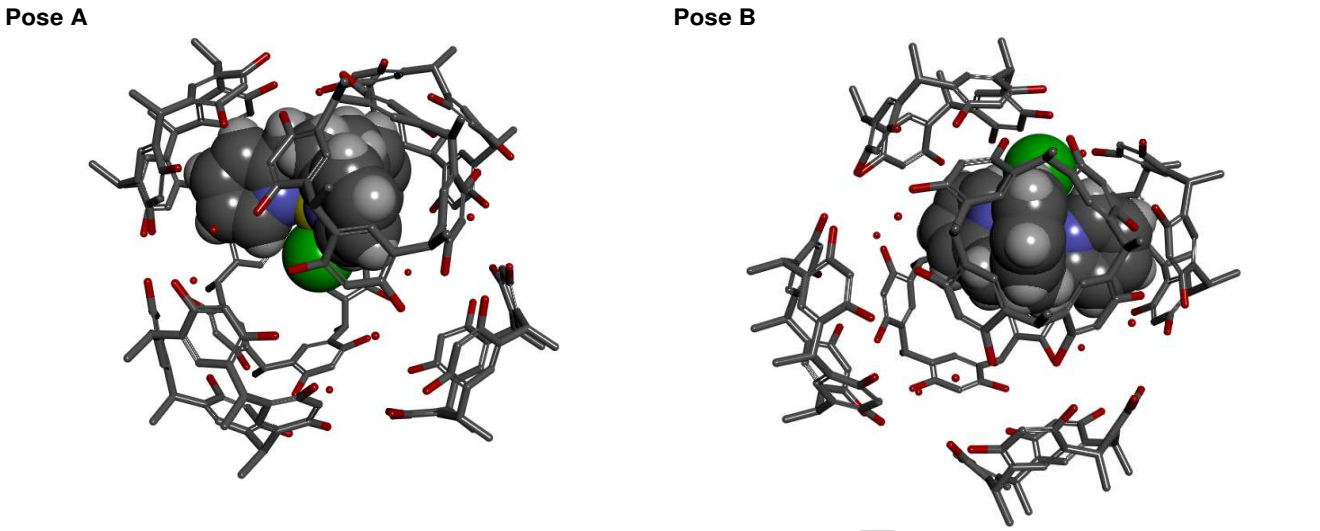

Figure 5. Binding poses A (left) and B (right) obtained by the docking of $[Zn(TMPA)Cl]^+$ in $\mathbf{1_6}$. Hydrogen atoms of the capsule are omitted for clarity.

points to the centre of the capsule and the 3 pyridine rings of the cation are buried in the cavities of 3 resorcinarenes with possibly multiple CH-π interactions. The three methylene groups are in close contact with a water molecule and 2 hydrogen bonds $CH\cdots OH_2$ are present ($d_{O\text{-}H}$ = 2.41 Å). In this pose, the protons H_3 and H_4 are closer to the shielding zones than any other protons of the complex. In the second pose (pose B Figure 5 right and Figures S55 and S56), the Zn-Cl vector points to the region of a water molecule but this water molecule is not engaged in a hydrogen bond with the chloride. Two pyridine rings are positioned in two resorcinarene cavities and the closest contacts are made by the protons H_4 and H_5.

The two binding poses obtained are in agreement with the splitting pattern observed in the ^{1}H NMR spectrum of **[Zn(TMPA)Cl-Cl@1$_6$]** in which the chloride counter-anion is also co-encapsulated (Figure 3). The packing coefficient (PC) for the cation $[Zn(TMPA)Cl]^+$ inside $\mathbf{1_6}$ is 0.32, well below the 0.55 ideal value proposed by Rebek and Mecozzi[43] and leaves some room for the co-encapsulation of up to three chloroform molecules (in the absence of the anion) in agreement with the experimental data obtained with the complex **[Zn(TMPA)Cl]BArF** (see Figures S57 and S58 for the docking of the complex in the two poses in presence of 3 co-encapsulated $CHCl_3$ molecules). Also, if at first glance, pose A seems to match better the CIS values, additional data related to the hydrogen bond donor capability of the capsule challenge this interpretation (*vide infra*).

Stability of the host-guest complex

The thermodynamic stability of the host-guest assembly **[Zn(TMPA)Cl@1$_6$]BArF** could not be directly assessed by NMR since a 1:1 mixture of **[Zn(TMPA)Cl]BArF** and $\mathbf{1_6}$ yields a quantitative encapsulation. We therefore conducted a competition experiment between the TMPA metal complex and tetrabutylammonium chloride. This guest forms a stable complex with $\mathbf{1_6}$ ($K > 10^4$ M^{-1}).[38] Thus, a 3 mM solution of **[NBu$_4$-Cl@1$_6$]** was prepared by dissolving a 1:1 mixture of the two initial species in water-saturated $CDCl_3$. The full encapsulation of the ammonium salt could be observed by ^{1}H NMR with the presence of resonances in the negative region of the spectrum and the absence of resonance for the free ammonium cation. One equivalent of **[Zn(TMPA)Cl]BArF** was then added. After equilibration of the solution at 50 °C for 12h, the ^{1}H NMR spectrum dramatically changed (Figure S48). This change is obvious when the fate of the ammonium cation is followed. Indeed, the intensity of the peaks in the negative region is strongly reduced at the expense of new peaks (for instance at ~3 ppm) corresponding to the free ammonium. This difference is due to the replacement of the ammonium guest by the TMPA complex in $\mathbf{1_6}$ (*vide supra* for the full characterisation of **[Zn(TMPA)Cl-Cl@1$_6$]**). By integration, more than 95 % of the initial guest was replaced, indicating a thermodynamic constant for this exchange higher than 10^2 and a very high stability constant of the assembly **[Zn(TMPA)Cl@1$_6$]** ($K > 10^6$ M^{-1}).

Second coordination sphere effect

Model complexes based on the TMPA ligand are encapsulated within the hexameric capsule and some space remains vacant for the co-encapsulation of other guest molecules. The separation of the complex from the bulk solvent and the control of the in⇆out exchange is reminiscent of the roles of the protein backbone in metalloenzymes. Another important role played by the amino acid residues found in the enzymatic pocket is to provide a second coordination sphere able to stabilise reactive intermediates. The second coordination sphere often consists in the presence of hydrogen bonding sites around the metal centre. In the capsule $\mathbf{1_6}$, it was shown that among the 8 water molecules embedded in the structure, four of them feature a hydrogen atom hanging inside the cavity which turns them into good hydrogen-bond donor sites.[44,45] In order to probe if capsule $\mathbf{1_6}$ could offer such a biomimetic second coordination sphere for the TMPA complex, we studied the encapsulation of two azido

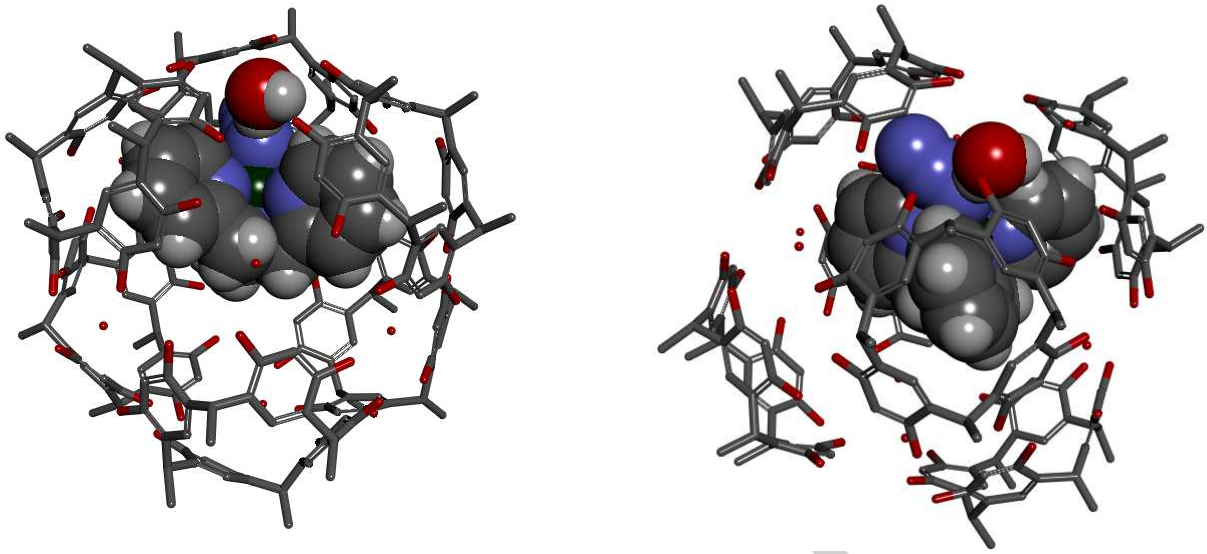

Figure 6. Two views of the same binding pose B' obtained by the docking of $[Cu(TMPA)N_3]^+$ in **1_6**. The water molecule hydrogen-bonded to N_3^- is represented in CPK style. Other hydrogen atoms of the capsule are omitted for clarity.

complexes, **[Zn(TMPA)N_3]ClO_4**, which could be studied by NMR and compared with the chloride complexes and **[Cu(TMPA)N_3]ClO_4**, which was previously reported as a reference to probe the second coordination sphere using Infra-Red (IR) spectroscopy.[46,47] In this matter, the coordinated azido ligand is a good reporter because its asymmetric $\nu_{N\text{-}N}$ stretching frequency shifts to a higher energy when the anion is hydrogen-bonded.[46,47] First, the Zinc complex was studied by NMR and the encapsulation of the azido complex was revealed by the cross-peaks visible in the COSY spectrum and further confirmed by the HSQC spectrum (Figures S49, S50 and S51). Three different sets of pairs of doublets for the CH_2 are present on the COSY spectrum pointing the presence of 3 isomeric capsular assemblies. The CIS due to the encapsulation of **[Zn(TMPA)Cl]ClO_4** and **[Zn(TMPA)N_3]ClO_4** are very close (Table S2). Once the encapsulation was confirmed by NMR, the extent of hydrogen-bonding within the capsule was investigated by examining the corresponding cupric complex by IR spectroscopy. The IR spectra of **[Cu(TMPA)N_3]ClO_4** and a 1:1.2 mixture of **[Cu(TMPA)N_3]ClO_4** and **1_6** were recorded in water-saturated $CHCl_3$. For the free complex, the asymmetric $\nu_{N\text{-}N}$ stretching band is found at 2047 cm^{-1} as previously reported.[47] This band is shifted by 12 cm^{-1} to a higher energy for the encapsulated complex (Figure S52). This experiment clearly demonstrates the presence of a hydrogen bond between the azido ligand and likely a water molecule of the capsule. The value of this shift also gives information about the strength of this hydrogen bond. For comparison, with hydrogen bond donor groups appended directly on the TMPA ligand, this value is + 10 cm^{-1} in the presence of one anilino group (-NH2) and + 17 cm^{-1} for the stronger pivalamido (-$HNC(O)C(CH_3)_3$) donating group.[47] The encapsulation of the cation $[Cu(TMPA)N_3]^+$ was further explored with docking simulation experiment. As for $[Zn(TMPA)Cl]^+$, two almost isoenergetic binding poses were obtained. The first pose A' is very similar to the pose A in the case of $[Zn(TMPA)Cl]^+$ (Figures S59, S60 and S61). The second pose B' shares some similarities with the pose B for $[Zn(TMPA)Cl]^+$ with the noticeable difference that a water molecule is now hydrogen bonded to the nitrogen atom of the azide bound to the copper cation (Figures 6 and S62). The short bond length of 1.52 Å is consistent with the strong H-bond revealed by IR spectroscopy. The existence of the hydrogen bond is clearly in contradiction with the pose A' which in turns is more strongly supported by the CIS value as in the case of the pose A for the cation $[Zn(TMPA)Cl]^+$. This seeming discrepancy is likely due to the fact that the docking simulation gives a frozen picture of the host-guest complex while the studies in solution embrace the many spatial arrangements adopted by the complex within the capsule.

Deprotonation of the capsular assembly

Capsule **1_6** has a high average acidity (p*K*a ≈ 5.9 with a microenvironmental p*K*a of ≈ 2.5).[45,48] **1_6** can be deprotonated by trialkylamine bases NR_3. Depending on the alkyl group R, the formation of the deprotonated capsule **$(1_6\text{-}H)^-$** is accompanied to some extent by the encapsulation of the ammonium.[48] The deprotonation yields an ion pair $[R_3NH^+@(\mathbf{1_6\text{-}H})^-]$ in which the cation is surrounded by its anion. The deprotonation of 3 host-guest complexes formed between **1_6** and **[Zn(TMPA)Cl]X** (**X** = **ClO_4**, **BArF** and **$(ZnCl_4)_{1/2}$**) was first investigated with $NOct_3$. In each case, the addition of 1.2 eq of base was rapidely (10 min at room temperature) followed by the deprotonation of the capsule. This could be observed in the ^1H NMR spectra with the disappearance of the peaks due to H_2O and the phenolic protons OH and the low field chemical shift for the methylene protons of the amine next to the nitrogen atom (Figures S63, S64 and S65). As it was previously reported (see for instance the effect of the base on the capsule alone, Figure S66), these modifications of the spectrum indicate the concomitant protonation of the amine and deprotonation of the capsule.[48] In addition, the 3 spectra, regardless the initial counter-anion present, are very similar (Figure S67). Upon deprotonation,

the initial capsular assemblies are likely transformed into the same host-guest species **[Zn(TMPA)Cl⁺@(1₆-H)⁻]** in which the cation is encapsulated in its own counter-anion. It also implies that upon deprotonation, the co-encapsulated chloride anion is expelled out of the capsule. The characterisation of the host-guest assembly was hampered by its instability in these conditions. Indeed, some signals in the negative region of the spectrum emerged when the samples were kept at room temperature for several hours. By heating the solutions at 50 °C for 18h, a stable final state could be reached (Figures S68). The rise of the new peaks between 0 and -2 ppm is detrimental to the signals for the free ammonium and very likely corresponds to the encapsulation of Oct_3NH^+. To solve this problem, another base that, in its protonated form, cannot compete as a guest for **1₆** was tested. We first checked that the deprotonation of the capsule **1₆** was effective with 1 eq of NaO^{t}Bu. After 2h at 50 °C, the expected modifications were observed on the ^{1}H NMR spectrum (Figure S69). Then, to the capsular assembly **[Zn(TMPA)Cl@1₆]ClO₄** was added 1 eq of NaO^{t}Bu. The resulting ^{1}H NMR spectrum with this base was identical to the one obtained immediately after the addition of $NOct_3$ (Figures S70 and S71). Heating the sample at 50 °C for several hours did not modify the spectrum. The encapsulation of the cation [Zn(TMPA)Cl]⁺ within the deprotonated anionic capsule **(1₆-H)⁻** was confirmed by the analysis of the HSQC and COSY NMR spectra and the peaks of the ^{1}H NMR spectrum could be assigned (Figures 7 and S72).

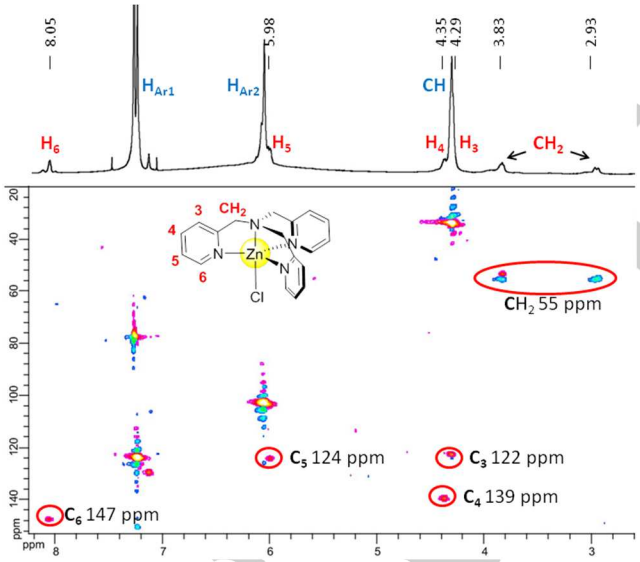

Figure 7. ^{1}H and HSQC NMR spectrum (water-saturated $CDCl_3$, 300 K, 500 MHz) of a 1:1 mixture at 3 mM of **[Zn(TMPA)Cl]ClO₄** and capsule **1₆** 2h at 50°C after the addition of 1 eq of NaO^{t}Bu.

The CIS of the protons of the complex upon encapsulation as **[Zn(TMPA)Cl@1₆]ClO₄** and **[Zn(TMPA)Cl⁺@[1₆-H]⁻]** do not differ (Table S3). The average position of the cation [Zn(TMPA)Cl]⁺ within the capsule is only marginally affected by the deprotonation.

The deprotonated capsule is an amphoteric species. It provides simultaneously in the direct environment of the metal coordination sphere acidic sites and one basic site. This basic site is probably delocalised over the 48 phenolic groups and 8 water molecules. Together with the second coordination sphere, the presence of an acid base dyad is a common feature in metalloenzymes. The biomimetic model proposed in this work shares this structural property. We finally examine the persistence of the hydrogen bonding capability in the second coordination sphere within the deprotonated capsule. To do that, we repeated the IR experiment with the assembly between **[Cu(TMPA)N₃]ClO₄** and **1₆** in presence of 1.5 eq of $NOct_3$. The IR spectra were recorded 10 minutes after the addition of the base to avoid the replacement of the encapsulated complex by the ammonium cation as observed by NMR. For the complex in solution or the complex encapsulated within **1₆**, the addition of the base did not change the position of the asymmetric $\nu_{N=N}$ stretching band (Figure S73). The shift due to the encapsulation keeps the same value of + 13 cm^{-1}. The azide anion thus remains hydrogen-bonded to one water molecule of the capsule and the deprotonation does not weaken the strength of this interaction.

Conclusion

The mononuclear [M(TMPA)A]⁺ cation (M = Zn^{II} or Cu^{II}, A = anionic ligand) is encapsulated within the hexameric capsular assembly **1₆** made of 6 resorcin[4]arenes and 8 water molecules with a high thermodynamic driving force ($K > 10^6$ M^{-1}). The full encapsulation is observed in presence of four different counter-anions, from a large and non-coordinating counter-anion ($BArF^-$) to smaller anions (halides). Some counter-anions are co-encapsulated (halides, triflate) while with $BArF^-$, the co-encapsulation of the anion is not observed and 3 $CHCl_3$ molecules are present in the capsule together with the cationic complex. The BArF counter-anion also leads to a much slower encapsulation showing that the nature of the counter-anion tunes the kinetic stability of the cation within the capsule. The co-encapsulated molecules can be exchanged without affecting the presence of the complex inside the capsule. For instance, the chloride anion can be replaced by the triflate anion. The analysis of the ^{1}H CIS also shows that the nature of the counter-anion does not modify the average position of the cation within the capsule but alters its tumbling motion. The position of the TMPA complex inside the capsule could be derived from an NMR analysis and was confirmed by docking simulations. Interestingly, in presence of a base, the capsule can be deprotonated. The resulting anionic capsule remains a host for the cation and provides acidic sites and a delocalised basic site in close proximity to the metal centre. Beyond the isolation of the complex from the bulk solvent, the capsule, in its neutral and anionic forms, also provides a secondary coordination sphere exemplified by the existence of a hydrogen bond between a water molecule and an azido ligand. The presence of this hydrogen bond was demonstrated by IR spectroscopy and confirmed with docking experiments.

Previous studies showed that the capsule **1₆** could control the nuclearity of a gold carbene complex by selecting the encapsulation of the mononuclear species.[22] The PC value for [Zn(TMPA)Cl]⁺ is 0.32 which does not allow for the encapsulation of putative dimeric species. This strategy is therefore very-well suited for the study of mononuclear reactive adducts. It was also

previously demonstrated that the in ⇆ out exchange was controlled by two factors. The primary factor is linked to the dynamics of the capsule itself. It involves the rupture of several hydrogen bonds, the dissociation of one resorcinarene unit with ($\Delta G^{\circ\neq} \approx 67$ kJ.mol^{-1}) and ultimately, the formation of a portal for the guest. The secondary factor reflects the passing of the guest through this portal. It depends on the guest and introduces size discrimination in this system. For example, it was measured that the activation barrier for tetrahexylammonium was ≈ 10 kJ.mol^{-1} higher than for tetrapropylammonium.[38] Therefore, this exchange mechanism not only permit a kinetic discrimination between the complex itself and the solvent molecules or anions, as it is observed in this work, but should also favor the exchange of co-encapsulated reagent, substrate or product molecules.

The high efficiency of metalloenzyme catalysts is mainly due to several structural features provided by the anchoring of a metal complex in a well-defined enzyme pocket: i) control of the nuclearity of the complex, ii) control of the access to the metal centre for the substrates and reactants and release of the products, iii) pre-organisation of the catalyst and the substrate, iv) stabilisation of intermediates and transition states by a second coordination sphere and v) control of the reactivity with the presence of acid-base residues. The host-guest complexes presented in this work gather some of these structural characteristics. For all these reasons, we believe that rather simple complexes, such as TMPA-based complexes, encapsulated within molecular cage $\mathbf{1_6}$ hold great promise not only as structural but also as reactive biomimetic models. This strategy offers a synthetically simple procedure to study rather sophisticated biomimetic systems and can be extended to the structurally closely related hexameric pyrogallol[4]arene capsule.[49,50] Future works in these directions will be pursued in our laboratory.

Experimental Section

Synthetic procedures, characterisation of the compounds and additional NMR and IR spectra are available in the Supporting Information.

Acknowledgements

This work was supported by Université de Paris with an IDEX grant ”Emergence en recherche”. We acknowledge the Macromolecular Modeling Platform at the Université de Paris for docking experiments.

Keywords: Bioinorganic • Resorcinarene capsule • Enzyme model • Host-Guest Chemistry

[1] For special issues on bio-inorganic enzymology: a) *Chem. Rev.* **1996**, *96*, 2237-3042; b) *Bioinorganic Enzymology II* **2014**, *114*, 3367-4038.

[2] For a virtual issue on Models of Metalloenzymes: *Inorg. Chem.* **2013**, https://pubs.acs.org/page/vi/2013/models-of-metalloenzymes.html.

[3] C. Würtele, E. Gaoutchenova, K. Harms, M. C. Holthausen, J. Sundermeyer, S. Schindler, *Angew. Chem. Int. Ed.* **2006**, *45*, 3867-3869.

[4] Y. Kobayashi, K. Ohkubo, T. Nomura, M. Kubo, N. Fujieda, H. Sugimoto, S. Fukuzumi, K. Goto, T. Ogura, S. Itoh, *Eur. J. Inorg. Chem.* **2012**, 4574-4578.

[5] S. Paria, Y. Morimoto, T. Ohta, S. Okabe, H. Sugimoto, T. Ogura, S. Itoh, *Eur. J. Inorg. Chem.* **2018**, 1976-1983.

[6] W. D. Bailey, D. Dhar, A. C. Cramblitt, W. B. Tolman, *J. Am. Chem. Soc.* **2019**, *141*, 5470-5480.

[7] R. L. Peterson, R. A. Himes, H. Kotani, T. Suenobu, L. Tian, M. A. Siegler, E. I. Solomon, S. Fukuzumi, K. D. Karlin, *J. Am. Chem. Soc.* **2011**, *133*, 1702-1705.

[8] M. Bhadra, J. Y. C. Lee, R. E. Cowley, S. Kim, M. A. Siegler, E. I. Solomon, K. D. Karlin, *J. Am. Chem. Soc.* **2018**, *140*, 9042-9045.

[9] J. Steinreiber, T. R. Ward, *Coord. Chem. Rev.* **2008**, *252,* 751-766.

[10] F. Yu, V. M. Cangelosi, M. L. Zastrow, M. Tegoni, J. S. Plegaria, A. G. Tebo, C. S. Mocny, L. Ruckthong, H. Qayyum, V. L. Pecoraro, *Chem. Rev.* **2014**, *114,* 3495-3578.

[11] N. Duchemin, I. Heath-Apostolopoulos, M. Smietana, S. Arseniyadis, *Org. Biomol. Chem.* **2017**, *15*, 7072-7087.

[12] J.-N. Rebilly, B. Colasson, O. Bistri, D. Over, O. Reinaud, *Chem. Soc. Rev.* **2015**, *44*, 467-489.

[13] L. J. Jongkind, X. Caumes, A. P. T. Artendorp and J. N. H. Reek, *Acc. Chem. Res.*, 2018, **51**, 2115.

[14] S. H. A. M. Leenders, R. Gramage-Doria, B; de Bruin, J. N. H. Reek, *Chem. Soc. Rev.* **2015**, *44*, 433-448.

[15] a) S. Horiuchi, T. Murase, M. Fujita *J. Am. Chem. Soc.* **2011**, *133*, 12445-12447; b) S. Horiuchi, T. Murase, M. Fujita, *Angew. Chem., Int. Ed.* **2012**, *51*, 12029-12031.

[16] D. Fiedler, D. H. Leung, R. G. Bergman, K. N. Raymond, *Acc. Chem. Res.* **2005**, *38*, 351-360.

[17] Z. J. Wang, C. J. Brown, R. G. Bergman, K. N. Raymond, F. D. Toste, *J. Am. Chem. Soc.* **2011**, *133*, 7358-7360.

[18] D. M. Kaphan, M. D. Levin, R. G. Bergman, K. N. Raymond, F. D. Toste, *Science* **2015**, *350*, 1235-1238.

[19] T. A. Bender, M. Morimoto, R. G. Bergman, K. N. Raymond, F. D. Toste, *J. Am. Chem. Soc.* **2019**, *141*, 1701-1706.

[20] L. R. MacGillivray, J. R. Atwood, *Nature* **1997**, *389*, 469-472.

[21] A. Carvazan, A. Scarso, P. Sgarbossa, G. Strukul, J. N. H. Reek, *J.* Am. *Chem. Soc.* **2011**, *133*, 2848-2851.

[22] L. Adriaenssens, A. Escribano-Cuesta, A. Homs, A. M. Echavarren, P. Ballester, *Eur. J. Org. Chem.* **2013**, 1494-1500.

[23] T. Omagari, A. Suzuki, M. Akita, M. Yoshizawa, *J.* Am. *Chem. Soc.* **2016**, *138*, 499-502.

[24] A. G. Blackman, *Eur. J. Inorg. Chem.* **2008**, 2633-2647.

[25] I. E. Philip, A. E. Kaifer, *J. Am. Chem. Soc.* **2005**, *70*, 1558-1564.

[26] I. E. Philip, A. E. Kaifer, *J. Org. Chem.* **2002**, *124*, 12678-12679.

[27] N. K. Beyeh, M. Kogej, A. Ahman, K. Rissanen, C. A. Shalley, *Angew. Chem., Int. Ed.* **2006**, *45*, 5214-5218.

[28] G. Bianchini, A. Scarso, G; La Sorella, G. Strukul, *Chem. Commun.* **2012**, *48*, 12082-12084.

[29] S. Horiushi, H. Tanaka, E. Sakuda, Y. Arikawa, K. Umakoshi, *Chem. Eur. J.* **2016**, *22*, 17533-17537.

[30] C. Gaeta, C. Talotta, M. De Rosa, P. La Manna, A. Soriente, P. Neri, *Chem. Eur. J.* **2019**, *25*, 4899-4913.

[31] Y. Cohen, S. Slovak, L. Avram Hydrogen Bond Hexameric Capsules: Structures, Host-Guest Interactions, Guest Affinities, and Catalysis. In *Calixarenes and Beyond* (Eds: P. Neri, J. L. Sessler, M.-X. Wang), Springer International Publishing, Cham, **2016**; pp. 811-842.

[32] R. R. Jacobson, Z. Tyeklar, A. Farooq, K. D. Karlin, S. Liu, J. Zubieta, *J.* Am. *Chem. Soc.* **1988**, *110*, 3690-3692.

[33] C. X. Zhang, S. Kaderli, M. Costas, E. Kim, Y.-M. Neuhold, K. D. Karlin, A. D. Zuberhüler, *Inorg. Chem.* **2003**, *42*, 1807-1823.

[34] M. A. Thorseth, C. S. Letko, E. C. M. Tse, T. B. Rauchfuss, A. A. Gewirth, *Inorg. Chem.* **2013**, *52*, 628-634.

[35] M. Asahi, S. Yamazaki, S. Itoh, T. Ioroi, *Electrochimica Acta*, **2016**, 211, 193-198.

[36] Q. Zhang, L. Catti, V. R. I. Kaila, K. Tiefenbacher, *Chem. Sci.* **2017**, *8*, 1653-1657.

[37] S. Merget, L. Catti, G. Piccini, K. Tiefenbacher, *J.* Am. *Chem. Soc.* **2020**, *142*, 4400-4410.

[38] Yamanaka, A. Shivanyuk, J. Rebek, Jr., *J. Am. Chem. Soc.* **2004**, *126*, 2939-2943.

[39] A. Shivanyuk, J. Rebek, Jr., *J. Am. Chem. Soc.* **2003**, *125*, 3432-3433.
[40] The position of the peak for water is also different. This is due to the different concentrations 1 mM vs. 3 mM. The same spectrum at 3 mM was also recorded and all the resonances were identical.
[41] The CIS for CH_2 are different but this difference mainly comes from the chemical shifts in the two free complexes: 3.89 ppm for **[Zn(TMPA)Cl@1$_6$]BArF** and 4.71 ppm for **[Zn(TMPA)Cl-Cl@1$_6$]**.
[42] LigandFit is implemented in Biovia Discovery Studio 2016. See C. M. Venkatachalam, X. Jiang, T. Oldfield, M. Waldman, *J. Mol. Graph. Model* **2003**; *21*, 289-307.
[43] S. Mecozzi, J. Jr. Rebek, *Chem. Eur. J.* **1998**, *4*, 1016-1022.
[44] P. La Manna, M. De Rosa, C. Talotta, C. Gaeta, A. Soriente, G. Floresta, A. Rescifina, P. Neri, *Org. Chem. Front.* **2018**, *5*, 827-837.
[45] P. La Manna, C. Talotta, G. Floresta, M. De Rosa, A. Soriente, A. Rescifina, C. Gaeta, P. Neri, *Angew. Chem. Int. Ed.* **2018**, *57*, 5423-5428.
[46] M. A. Ehudin, A.W. Schaefer, S. M. Adam, D. A. Quist, D. E. Diaz, J. A. Tang, I. Solomon, K. D. Karlin, *Chem. Sci.* **2019**, *10*, 2893-2905.
[47] D. E. Diaz, D. A. Quist, A. E. Herzog, A. W. Schaefer, I. Kipouros, M. Bhadra, E. I. Solomon, K. D. Karlin, *Angew. Chem. Inter. Ed.* **2019**, *58*, 17572-17576.
[48] Q. Zhang, K. Tiefenbacher, *J. Am. Chem. Soc.* **2013**, *135*, 16213-16219.
[49] T. Gerkensmeier, W. Iwanek, C. Agena, R. Frohlich, S. Kotila, C. Nather, J. Mattay, *Eur. J. Org. Chem.* **1999**, 2257-2262.
[50] J. L. Atwood, L. J. Barbour, A. Jerga, *Chem. Commun.* **2001**, 2376-2377.

Table of Contents

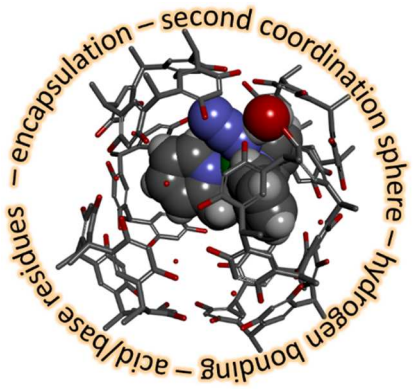

The encapsulation of a coordination complex in a dynamic hydrogen bonded capsule exhibits several features present in metalloenzyme such as the isolation of the metal centre from the bulk solvent while maintaining guest exchanges, a well-defined second coordination sphere and acid/base residues close to the metal centre.